Lab on a Chip

Cite this: *Lab Chip*, 2012, **12**, 4465–4471

www.rsc.org/loc

PAPER

A magnetic cell-based sensor†

Hua Wang,‡[ab] Alborz Mahdavi,‡[cd] David A. Tirrell[d] and Ali Hajimiri*[a]

Received 23rd April 2012, Accepted 13th August 2012
DOI: 10.1039/c2lc40392g

Cell-based sensing represents a new paradigm for performing direct and accurate detection of cell- or tissue-specific responses by incorporating living cells or tissues as an integral part of a sensor. Here we report a new magnetic cell-based sensing platform by combining magnetic sensors implemented in the complementary metal-oxide-semiconductor (CMOS) integrated microelectronics process with cardiac progenitor cells that are differentiated directly on-chip. We show that the pulsatile movements of on-chip cardiac progenitor cells can be monitored in a real-time manner. Our work provides a new low-cost approach to enable high-throughput screening systems as used in drug development and hand-held devices for point-of-care (PoC) biomedical diagnostic applications.

Introduction

There is an unmet need for high-throughput and cost-effective detection platforms for chemical and biological agents. These platforms can be utilized for a plethora of analytical and diagnostic applications including screening chemical libraries for drug development, toxicity studies, point-of-care (PoC) diagnostics, and environmental monitoring. Conventional sensors generally use chemical, optical, spectroscopic, electrical impedance- or mass-based detection to interpret biochemical phenomena. Cell-based sensing on the other hand makes use of living cells or tissues as an integral part of the sensor, and utilizes inherent cellular mechanisms to perform accurate detection of cell- or tissue-specific responses.[1–6] By providing both high sensitivity and specificity, cell-based sensing has tremendous potential for screening biochemical agents, particularly in the context of individualized medicine where effects often vary from patient to patient.[7,8] However, the applications of existing cell-based sensing platforms are often limited by detection mechanisms. For instance, optical detection, though useful in many applications, requires visible changes in cell morphology, a transparent medium, and analysis of cell images.[6] Moreover, existing cell-based sensors typically need dedicated device fabrication processes, which have low scalability and suffer from low yields in manufacturing. On the other hand, integrated electronic technology is becoming a powerful and low-cost platform for implementing advanced sensors. In particular, the complementary metal-oxide semiconductor (CMOS) process, which is widely employed in manufacturing consumer electronics, such as microprocessors and memory chips, can be directly used to realize large biosensor arrays with high scalability at very low cost.[9–27] More importantly, standard CMOS supports magnetic sensing; it uses magnetic particles as sensing tags,[26,27] whose functionality is independent of the optical or electrical properties of the cells or the medium.[28,29] This strategy provides a robust platform for implementing cell-based sensors.

Here we seek to combine the benefits of CMOS technology with the advantages of cell-based sensing by developing a new detection platform based on a CMOS magnetic sensor with cardiac progenitor cells tagged by magnetic particles. We show that the cardiac progenitor cells can be differentiated directly on a CMOS integrated sensor chip to form a cell-based sensor, and that the periodic and autonomous beating of the progenitors can be detected in real-time by CMOS magnetic sensing. We further demonstrate that the sensor enables accurate detection of chemical agents. The approach described here can be readily utilized to construct low-cost and field-deployable biochemical sensors.

Methods and materials

We used cardiac progenitors, differentiated from mouse embryonic stem cells (ESCs), as the sensing cells. Cardiac progenitors beat autonomously and undergo displacements of tens of microns.[6] We designed and implemented a fully integrated inductive frequency-shift magnetic sensor array in a standard CMOS process.[27] With magnetic particles coated on the cells, the beating movements of the cardiac progenitors can be accurately captured by the CMOS magnetic sensors without any post-processing of the data (Fig. 1). If the analyte of interest alters the physiology of the cells and subsequently their pulsatile

[a]*Department of Electrical Engineering, California Institute of Technology, Pasadena, CA 91125, USA. E-mail: hajimiri@caltech.edu*
[b]*School of Electrical and Computer Engineering, Georgia Institute of Technology, Atlanta, GA 30332, USA. E-mail: hua.wang@ece.gatech.edu*
[c]*Department of Bioengineering, California Institute of Technology, Pasadena, CA 91125, USA*
[d]*Division of Chemistry and Chemical Engineering, California Institute of Technology, Pasadena, CA 91125, USA*
† Electronic Supplementary Information (ESI) available: Supplementary figures for sensor noise cancellations, SEM images, mouse embryonic stem cells preparations, and sensor system diagram with the measurement setup. See DOI: 10.1039/c2lc40392g
‡ Both authors contributed equally to this paper.

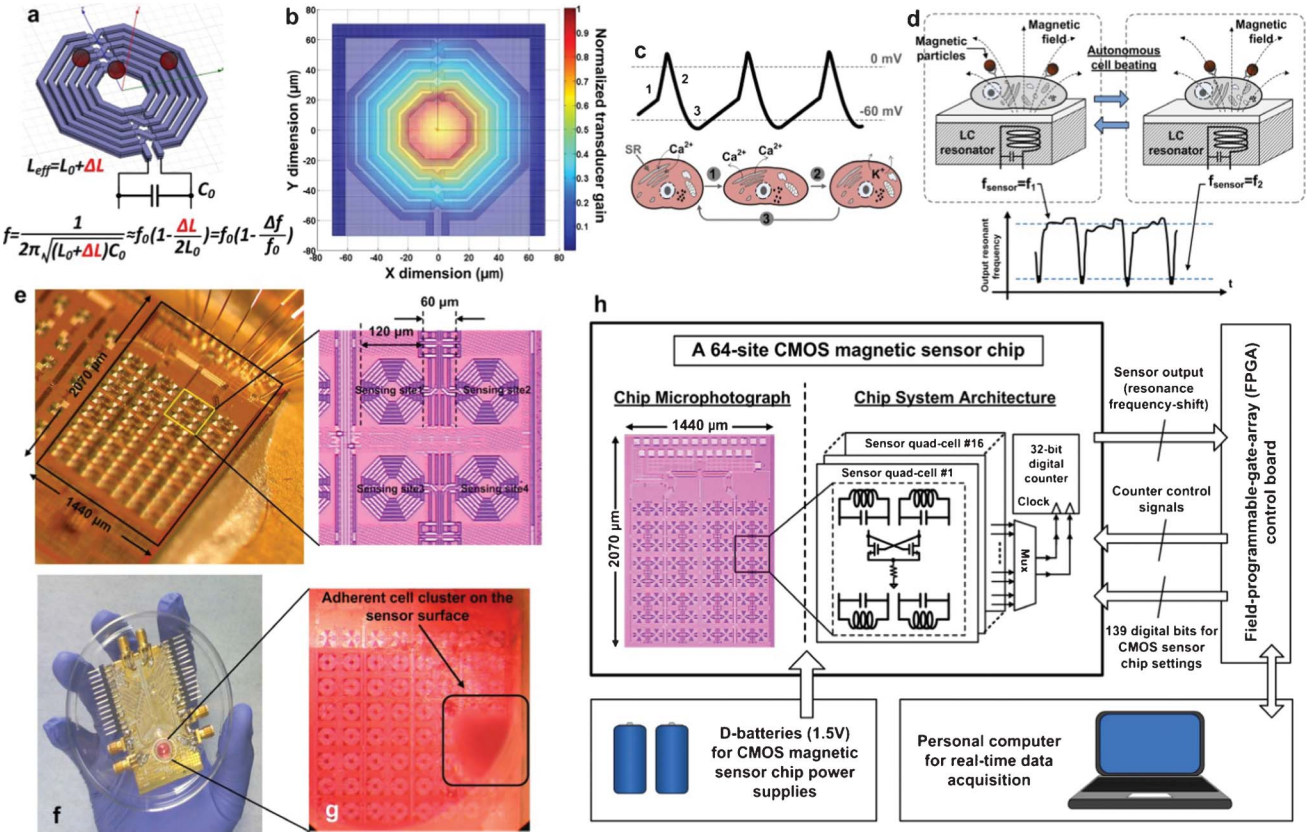

Fig. 1 Magnetic cell-based sensor. (a) Magnetic particles result in an increased effective inductance L_{eff} in the LC resonator, which causes a downshift in the resonant frequency. This frequency shift can be detected by the CMOS circuits and serves as the readout for the sensing unit. (b) The normalized transducer gain (sensitivity to magnetic particles) of the CMOS magnetic sensor is plotted with respect to the sensor inductor geometry. (c) A spontaneous cardiac cell beating. Inset at top shows the cell potential changes (in milli-volts) during the periodic beating motion. SR = sarcoplasmic reticulum. (d) Autonomous beating of the cardiac progenitor cells leads to displacements of the magnetic particles and is detected by the CMOS magnetic sensor as periodic shifts in resonant frequency. (e) The sensor chip contains 64 (8 × 8) independent sensing sites as a sensor array. A zoom-in view shows the individual sensing site. (f) The sensor module fits in a petri dish. The module includes a PDMS reservoir to hold the cardiac progenitor cells and the medium. (g) An image of the PDMS sample reservoir shows a cell cluster on the CMOS sensor surface. (h) Diagram for the CMOS magnetic sensor chip microphotograph, chip system architecture, and the measurement setup.

movements, the changes are readily recorded by the sensor in real-time.

Preparation of the cardiac progenitor cells

Culturing cardiac progenitors from mouse ESCs. R1 mouse embryonic stem cells (ESCs) were obtained from ATCC and propagated in ESC maintenance medium supplemented with leukemia inhibitory factor (LIF) to maintain their undifferentiated state. The ESC maintenance medium consists of Dulbecco's Modified Eagle's Medium containing 15% of ES qualified fetal bovine serum (FBS) (16141-061; Gibco), 100 μM β-mercaptoethanol (M6250; Sigma-Aldrich), 2 mM L-glutamine (25030-081; Invitrogen Inc.), 0.1 mM nonessential amino acids (11140-050; Invitrogen Inc.), 1 mM sodium pyruvate (11360-070; Invitrogen Inc.), 50 U mL^{-1} penicillin and 50 μg mL^{-1} streptomycin (15140-122; Invitrogen Inc.). We supplemented the ESC maintenance medium with 500 pM murine leukemia inhibitory factor (LIF) (ESG1107; Millipore). Differentiation medium had an equivalent composition to ESC maintenance medium but lacked LIF. We cultured mouse ESCs routinely on 0.2% gelatin-coated tissue-culture flasks and trypsinized them with 0.05% Trypsin-EDTA (25300062; Gibco) for passaging purposes. Embryoid bodies (EBs) were made from these cells by the hanging drop technique.[30] Mouse ESCs of passage number 15–20 were used. Differentiation was initiated by resuspension in differentiation medium lacking LIF. Cells were resuspended at a density of 500 cells per 20 μL of medium for the hanging drops. Each hanging drop contained 20 μL of cell suspension.

Direct EB differentiation on the CMOS sensor surface. In order to yield pulsatile cardiac progenitor cells with high viability and reliable attachment to the magnetic sensor, we directly differentiated ES cells on the CMOS sensor surface. To minimize contamination, we first rinsed the chip surface as well as the PDMS reservoir with 100% ethanol and PBS before surface modification. Since standard CMOS processes use silicon nitride as the top passivation layer, to enhance cell attachment to the silicon nitride surface, we coated the active sensing area (the 64 sensing sites) with 12.5 μg mL^{-1} fibronectin (F1141; Sigma) in 0.02% gelatin at 37 °C and 5% CO_2 for 24 h.[31,32] The fibronectin coating allows integrin receptors on the cell membrane to bind to the surface, localizes the cells to the active sensing area, and

increases their adhesion to the sensor. Although the sensor can be used with cells in suspension, surface attachment of cells to the sensor area provides for a robust signal by making sure that small movements of the entire assembly are not registered as cell movements and that the cells are optimally positioned on the sensor coils for maximum signal. We seeded the EBs onto the sensor and incubated the entire assembly at 37 °C and 5% CO_2 for ten days in differentiation medium lacking LIF. The medium was replaced every 24 h. During this time, the EBs proliferated, attached to the sensor surface, and formed micro-tissues consisting of cardiac progenitors. The presence of cardiac progenitors, which formed spontaneously in differentiation medium, was visually verified.

Coating the cells with magnetic particles. We coated the cardiac progenitor cells with micron-sized magnetic particles (D = 2.4 μm) to track their pulsatile movements. We used epoxy functionalized magnetic beads (Dynabead M-270; Invitrogen Inc). In order to enhance bead attachment to cells, the magnetic beads were functionalized with fibronectin (F1141; Sigma) by using an epoxy functionalization kit according to the manufacturer's recommendations (Dynabead M-270; Invitrogen Inc). After 30 min of attachment, excess beads were removed with three sequential medium changes. Bead attachment to the surface of the cells was observed visually by using a stereo microscope; subsequent medium changes did not alter bead positions. Visual inspection of the cells showed that on average 10 beads were attached to each cell.

CMOS magnetic sensor for real-time monitoring of cell beating

CMOS magnetic sensor and its implementation. The core of the CMOS magnetic sensor is an on-chip inductor-capacitor (LC) resonator.[26] When magnetic particles are present, they increase the total magnetic energy in the space, lead to a change in the effective inductance in the resonator, and result in a resonant frequency down-shift (Fig. 1a). The frequency-shift per magnetic particle can be modelled as the sensor transducer gain and is designed to present high spatial non-uniformity in our LC sensing resonator (Fig. 1b). Changes in the cell shape or position during the sensing process directly cause redistribution of the attached particles. This spatial distribution leads to variation in the total resonant frequency-shift and is readily detected by the CMOS sensor in real-time. Thus, for the autonomous beating of the cardiac cells in this study, the resulting magnetic sensor output is a series of periodic pulses (Fig. 1c and 1d). To achieve a sub-part-per-million (10^{-6}) relative frequency-shift sensitivity, we implemented a low noise on-chip oscillator with Correlated-Double-Counting (CDC) noise suppression technique for each LC resonator as the read-out circuits on the CMOS chip.[27] The sensor's magnetic sensitivity is limited by the noise in the CMOS electronics. The sensor is capable of detecting a single micron-size magnetic bead;[27] therefore even with very small numbers of beads on cells, the system is able to detect movement of the cells.

We implemented a magnetic sensor array with 64 independent sensing sites by paralleling 16 quad-core sensor units each with 4 independent on-chip magnetic sensor sites[27] (Fig. 1e). Each sensor site occupies an area of 120 μm by 120 μm, which is conducive to cell- or tissue-level detection. By adding more sensing sites, this architecture enables straightforward extension to very-large-scale sensor arrays for high throughput applications, where massively paralleled testing can be used for characterizing different cell types and testing different chemicals simultaneously.

The sensor inductor optimization was achieved by using Ansoft HFSS™ V11 and Ansoft Maxwell® V10. The CMOS sensor chip integrated circuits were designed using the Cadence® Design System as the Electronic Design Automation (EDA) software. The system's magnetic detection functionalities and the digital programmability and real-time data readout were verified by using simulators of SpectreRF® and Ultrasim®, respectively. Finally, we customized the sensor chip for a standard 65 nm CMOS process fabricated by United Microelectronics Corporation (UMC).

Assembly of the sensing module. We used a brass substrate as the base of the sensor module to provide good mechanical stability, low resistance thermal path, and electrical ground reference of the sensor chip. The Printed-Circuit-Board (PCB) was implemented using RT/Duroid® 6010 laminate material (Rogers Corporation) and was fabricated by DVH Circuit. We completed the attachment of the CMOS sensor chip, the PCB board, and the brass substrate by using silver epoxy (H20E, Epoxy Technology, Inc), which was cured after a 2 h baking at 120 °C. We then used gold wire-bonds to complete the sensor chip packaging and electrical connections.

In order to hold the sensing cells and the test chemicals, we constructed a polydimethylsiloxane (PDMS) reservoir on top of the CMOS sensor chip (Fig. 1f and 1g). GE Silicones® RTV 615 kit, as the PDMS raw material, was obtained from Applied Material Tech. We first mixed the PDMS base material and its curing agent at a 10 : 1 ratio to form the sealing material for the reservoir. Then, we constructed a cylindrical reservoir from a short piece of plastic tubing (D = 0.5 cm). The plastic reservoir was placed over the sensor chip and aligned with the sensing area. We used the PDMS as adhesive around the reservoir and thermally cured the entire assembly for one hour at 50 °C.

Preparation of the real-time data acquisition interface. To control the sensor chip operation and perform data acquisition, we used an Altera® DE2 board with Cyclone® II 2C35 FPGA core, which directly interfaced with the personal computer as the measurement console. This setting provides fully reprogrammable digital control signals, which were sent to the CMOS sensor chip to enable the operation of the desired magnetic sensor sites. The corresponding measured data were directly acquired also by the FPGA board and subsequently saved on the personal computer (Fig. 1h). Customized Verilog® codes were developed to operate the FPGA board.

Toxicity test of chemical agents

Two sets of chemical sensing experiments were performed to demonstrate the detection functionality of the magnetic cell-based sensor in this study. In the first set of experiments, extracellular ion concentrations were varied independently to test the corresponding beating frequency changes of the cardiac progenitor cells. In the second experiment, lidocaine (Sigma) was

used as a small molecule drug, whose effect on the cell beating amplitude was monitored. The test chemicals were prepared in the culture medium and directly introduced into the PDMS chambers on the CMOS magnetic sensors. Before each chemical was applied, the sensors registered the beating frequency or amplitude of the cardiac cells under the normal physiological condition for at least 5 min as the control measurements. These data were later used as the baseline values for normalization.

Results and discussion

Real-time chemical detection

The magnetic beads were attached to the cardiac progenitor cells as a one-step preparation procedure before the test chemicals were introduced and remained bound throughout the measurements. Since no further labelling is needed during the sensing process for either the sensor or the test chemicals, in this respect our sensor performs direct detection, similar to the previously invented method of optical detection of cardiac toxicity on chip.[6] Since the CMOS magnetic sensor directly outputs the beating frequency and amplitude of the cardiac cells, no post-processing of data is required by our approach, which enables real-time monitoring during detection. These features of the method significantly simplify the sample preparation and sensing procedures, and facilitate highly parallel and low-cost biochemical screening.

Due to the autonomous beating of the cardiac progenitor cells, the output of the magnetic sensor is a series of periodic pulses, which we verified to match the beating of the cell cluster. The signal amplitude of the sensor output is proportional to the displacement in the pulsatile cell beatings, and the averaged period between pulses determines the beating frequency of the cell cluster. Since the cardiac cells beat with a frequency below 1 Hz in our experiments, we set the sensor sampling rate at 20 Hz to satisfy the Nyquist minimum sampling rate and ensure accurate amplitude peak recording for the pulsatile waveforms. As a typical control measurement on the cardiac progenitor cells' beating rate, we observed a frequency of 0.48 Hz under normal physiological conditions, *i.e.* with the extracellular potassium ion concentration of 3.4 mM (Fig. 2a and 2b).

In addition, we found that differentiation of the EBs directly on the CMOS sensor surface was more effective in yielding pulsatile cell clusters compared to seeding the clusters after off-chip differentiation. Physical disruption in the latter approach, *e.g.* with cell scrapers, could abrogate the clusters' synchronous motions. We maintained the cells on the sensor surface for up to 15 days without loss of viability or significant morphological changes. The sensor life-time can potentially be extended by frequent medium changes and accurate temperature control, which is important for in-field diagnostic sensors.

Toxicity test of extracellular potassium and calcium ions

Extracellular potassium and calcium ion concentrations have well-known and significant effects on action potential generation and thus on the autonomous beating activities of the cardiac cells. We used different concentrations of these ions for proof-of-concept testing of the magnetic cell-based sensor functionality. We dissolved potassium and calcium in the culture media and prepared the potassium test samples with concentrations of 3.4 mM (normal physiological concentration), 10 mM, and 20 mM and the calcium test samples with concentrations of 2 mM (normal physiological concentration), 4 mM, and 8 mM. The test chemicals were delivered into the PDMS reservoir by pipettes.

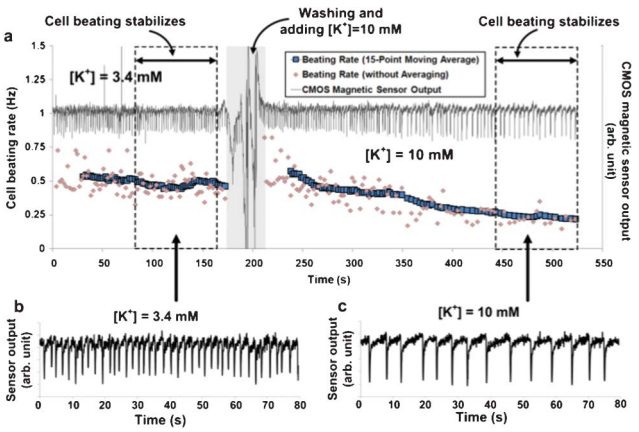

Fig. 2 Real-time sensor response when the extracellular potassium (K^+) level is increased. (a) The recorded sensor response and the corresponding change in the extracellular potassium level. The averaged cell beating rate stabilizes within 3 min after the K^+ level increase, which demonstrates a fast response time of the cell-based sensor. (b) Zoom-in plot of the stabilized sensor output in (a) at an extracellular K^+ level of 3.4 mM. (c) Zoom-in plot of the stabilized sensor output in (a) at an extracellular K^+ level of 10 mM. (b) and (c) show the steady state sensor outputs in (a).

We first increased the potassium concentration from normal physiological conditions (3.4 mM) to 10 mM and observed a corresponding decrease in the recorded pulse frequency from 0.48 Hz to 0.19 Hz (Fig. 2a and 2c). This result verifies that the recorded frequency shifts were indeed due to the pulsatile motions of the cardiac progenitors, and is in agreement with previously reported responses of spontaneously pulsating cardiac cells.[33,34] Since no labelling step was required, the measurement time was governed by the inherent response time of the cardiac progenitor cells. We observed a three minute response time to a shift in potassium ion concentration from 3.4 mM to 10 mM, which shows fast sample-in-answer-out detection capability.

Increases in the extracellular potassium concentration from 3.4 mM to 10 mM and then to 20 mM resulted in monotonically reduced pulse frequency until the cells stopped beating (Fig. 3a and 3b). In addition, we increased the extracellular calcium concentration from 2 mM to 4 mM and 8 mM, and measured increases in the pulsatile frequency of the cells by 27% and 46%, respectively (Fig. 3c and 3d). These observed trends were consistent with previously reported responses of cardiomyocytes.[33,34]

Finally, we tested the reversibility of the sensor to show that it can be restored to its nominal state and reused. We first increased the extracellular potassium concentration to 20 mM to stop the autonomous cell movement, and were able to recover the pulsatile motion by washing the sensor with the cell medium to return the potassium concentration to its normal physiological value of 3.4 mM (Fig. 4). In our measurement, two consecutive washes were needed to adjust the potassium concentration. This result suggests that the sensor can potentially be reused without

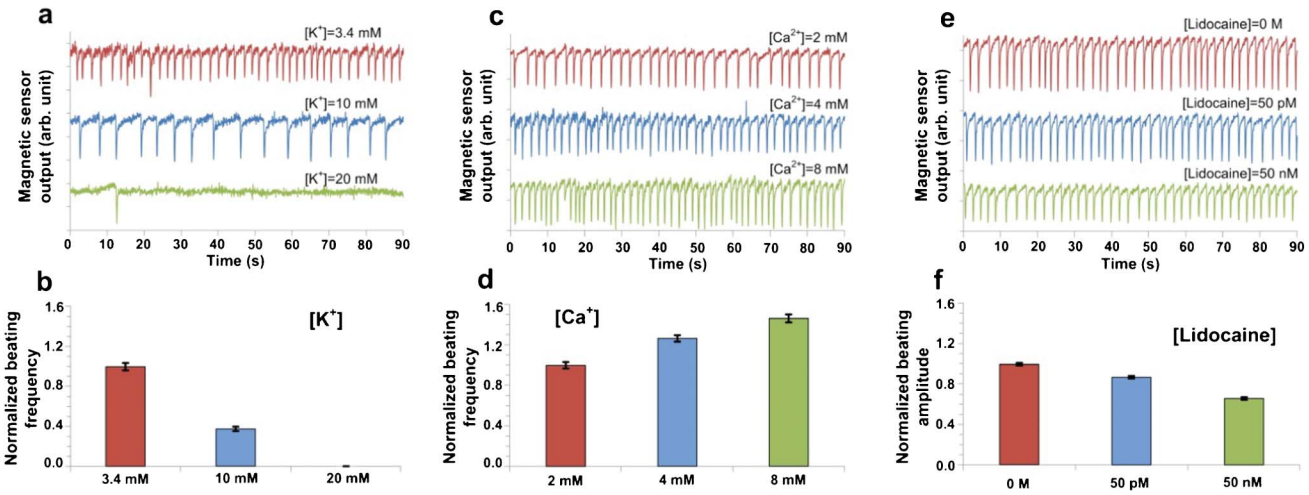

Fig. 3 Measurement of the magnetic cell-based sensor steady state outputs. (a) and (b) The real-time measured sensor output and the beating frequency summary when the cell clusters are subjected to changes in extracellular potassium concentration. Beating rate decreases with an increase in extracellular potassium level. (c) and (d) The real-time measured sensor output and the beating frequency summary when the cell clusters are subjected to extracellular calcium concentration changes. The cell pulsatile beating rate is accelerated when the extracellular calcium level is increased. (e) and (f) The real-time measured sensor output and the beating amplitude summary when lidocaine is added to the cell medium. The amplitude of the cell beating is reduced at a higher extracellular lidocaine concentration. Error bars represent standard errors.

loss of functionality, and further shows the robustness and potentially extended life-time of the sensor.

Small molecule detection

To test the functionality of the magnetic cell-based sensor in detecting small molecules, we used lidocaine as a test chemical. Lidocaine is a small molecule anti-arrhythmic drug that blocks fast-gated sodium ion channels, impedes the cells from depolarizing, and decreases the amplitude of the pulsatile motions. Due to its rapid onset of action, lidocaine is commonly used intravenously as an amino amide-type local anesthetic for the treatment of ventricular arrhythmias.[35]

We first dissolved lidocaine in cell culture medium at concentrations of 50 pM and 50 nM. The lidocaine test samples were then delivered into the sensor PDMS reservoir through pipettes. With increases in lidocaine concentration to 50 pM and then to 50 nM, the recorded cell beating amplitudes were reduced to 89% and 68% of the values observed without lidocaine (Fig. 3e and 3f). These observations were consistent with the mechanistic effect of lidocaine.[35]

The real-time recorded sensor output data in Fig. 5 shows the cell beating amplitudes with respect to time. We observed that the beating amplitudes were initially increased after the lidocaine samples were applied, potentially due to the temperature changes in the cell medium. The beating amplitudes then gradually slowed down and stabilized with increasing lidocaine concentration. The recorded response times were 10 min for 50 pM lidocaine and 13.8 min for 50 nM lidocaine. These short response times manifest the fast onset of the lidocaine toxicity effect and also demonstrate the fast detection capability of the magnetic cell-based sensor.

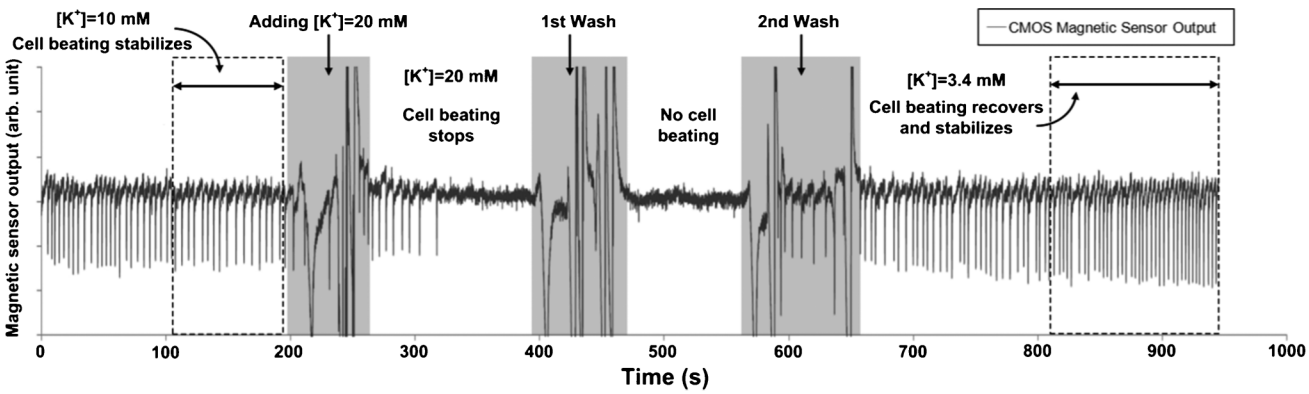

Fig. 4 Recovery test of the magnetic cell-based sensor. A real-time measured sensor output shows that the autonomous beating of the sensor cells can be restored. Cell beating stops when the extracellular potassium level is raised to 20 mM, and is then recovered after two washes with the medium containing 3.4 mM potassium ion. The steady state sensor outputs are highlighted in the boxed regions.

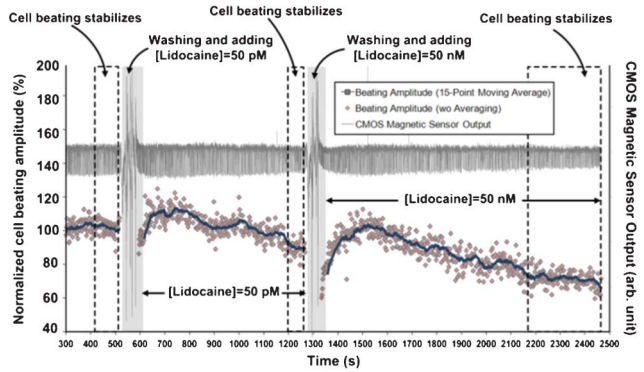

Fig. 5 Real-time recorded sensor response when lidocaine is introduced. A measured sensor output shows that the beating amplitude of the sensor cells decreases when increasing the extracellular lidocaine level. The cell beating amplitude at physiological condition is used as the baseline reference. Medium containing a lidocaine concentration of 50 pM is first added at t = 510 s. The sensor output stabilizes after 10 min with its normalized amplitude decreases to 89% of the baseline value. Then, medium containing 50 nM lidocaine is added at t = 1280 s. The sensor output stabilizes after 14 min, and the normalized beating amplitude decreases to 68% of the baseline value. The steady state sensor outputs are highlighted in the boxed regions.

Conclusions

We have demonstrated a magnetic cell-based sensor that combines the advantages of a low-cost CMOS microelectronics manufacturing process and a cell-based sensing scheme with cell- or tissue-specific responses. Existing biochemical sensing modalities are either incompatible with the CMOS manufacturing processes or are limited due to their detection requirements. For example, optical detection methods require visible changes in cell morphology, can be limited by photo-bleaching, and are difficult to integrate into compact system.[6,9,11] Electrochemical sensing is sensitive to electrical charge variations at the electrode-electrolyte interfaces, and thus experience significant signal drift and offset due to the measurement background.[18–20] In contrast, magnetic sensing offers unique advantages as a non-optical and non-contact detection scheme, avoiding all the aforementioned issues.[21–27] Moreover, since most biological samples and media are magnetically transparent, a low background noise level and reduced off-target effects are obtained.[28,29] More importantly, the CMOS magnetic sensor can be manufactured at low cost and for large production volumes.

Depending on the application of interest, our magnetic cell-based sensor can be outfitted with a variety of cell types with diverse functionalities. Mouse ESCs are particularly suitable for building high-throughput cell-based sensors in large volume, since they can be readily expanded to large numbers and differentiated to various cell types. The direct on-chip differentiation of mouse ESCs substantially simplifies the required preparation and handling steps, and further benefits mass production of the magnetic cell-based sensor.

In this study, the physical movement of the cardiac progenitor cells, *i.e.* pulsatile motion, was used as a robust detection signal; this movement could also take other forms, such as cell migration, for implementing similar cell-based sensing platforms. Moreover, sensor cells can be genetically modified to increase sensitivity and selectivity to certain chemical stimuli, thereby enhancing the functionality of the cell-based sensor.

Since this magnetic cell-based sensor does not require labelling during the measurement, it enables fast sample-in-answer-out chemical detection. Measurement times are limited only by the response time of the cells and can be as fast as three minutes as shown here. The long sensor life-time and high level of robustness should make these systems useful for in-field diagnostic applications. Cell proliferation may potentially be measured by this system by tracking long-term changes in positions of magnetic beads. Since cell proliferation occurs on time scales much longer than those of pulsatile motions, the sensor makes accurate measurements in the presence of cell proliferation. The most important limitations of this sensor technology arise from the need to maintain the sensing unit under physiological conditions.

Several implementation refinements can be made to the sensor to achieve a complete lab-on-chip system. A microfluidic structure can be easily included to standardize sample delivery and medium exchange, and to provide the parallel detection chambers required for high-throughput chemical screening.[26,36,37] Temperature regulators can be integrated into the CMOS circuit to accurately control the local or global thermal environment on the sensor,[26,38] and to extend the long-term viability of the sensor cells with no need for any external heating devices.

In conclusion, our magnetic cell-based sensing platform provides a compact solution for rapid and real-time detection of biochemical agents. Based on this method, it is possible to construct fully portable chemical sensors. This approach may greatly reduce the cost of high-throughput screening systems in drug development and also enable hand-held devices for point-of-care (PoC) diagnostic applications, such as epidemic disease control and environmental monitoring.

Acknowledgements

H. W. was supported by a California Institute of Technology Innovation Initiative (CI2) Research Grant. A.M. was supported by a National Science and Engineering Research Council of Canada (NSERC) Scholarship, a post-graduate scholarship by Caltech Donna and Benjamin M. Rosen Center for Bioengineering and the NSF Center for the Science and Engineering of Materials at Caltech (NSF DMR 0520565). The authors would like to acknowledge Dr Shouhei Kousai for his support on the CMOS magnetic sensor chip development; Constantine Sideris for his help on developing the FPGA Verilog programs; Alex Pai for his support on building the sensor modules; and United Microelectronics Corporation (UMC) for providing CMOS sensor chip foundry service.

References

1 S.V. Sharma, D.A. Haber and J. Settleman, *Nat. Rev. Cancer*, 2010, **10**, 241–253.
2 Y. Meng, A. Kasai, N. Hiramatsu, K. Hayakawa, K. Yamauchi, M. Takeda, H. Kawachi, F. Shimizu, J. Yao and M. Kitamura1, *Lab. Invest.*, 2005, **85**, 1429–1439.
3 P. Banerjee, D. Lenz, J. P. Robinson, J. L. Rickus and A. K. Bhunia, *Lab. Invest.*, 2007, **88**, 196–206.
4 T. H. Rider, M. S. Petrovick, F. E. Nargi, J. D. Harper, E. D. Schwoebel, R. H. Mathews, D. J. Blanchard, L. T. Bortolin, A. M. Young, J. Chen and M. A. Hollis, *Science*, 2003, **301**, 213–215.

5 J. J. Pancrazio, J. P. Whelan, D. A. Borkholder, W. Ma and D. A. Stenger, *Ann. Biomed. Eng.*, 1999, **27**, 697–711.
6 S. B. Kim, H. Bae, J. M. Cha, S. J. Moon, M. R. Dokmeci, D. M. Cropek and A. Khademhosseini, *Lab Chip*, 2011, **11**, 1801–1807.
7 T. Y. Chang, C. Pardo-Martin, A. Allalou, C. Wählby and M. F. Yanik, *Lab Chip*, 2012, **12**, 711–716.
8 C. Pardo-Martin, T. Y. Chang, B. K. Koo, C. L. Gilleland, S. C. Wasserman and M. F. Yanik, *Nat. Methods*, 2010, **7**, 634–636.
9 A. El Gamal and H. Eltoukhy, *IEEE Circuits Devices Mag.*, 2005, **21**, 6–20.
10 O. Graydon, *Nat. Photonics*, 2010, **4**, 668.
11 T. Huang, S. Sorgenfrei, K. L. Shepard, P. Gong and R. Levicky, *IEEE J. Solid-State Circuits*, 2009, **44**, 1644–1654.
12 K. K. Ghosh, *Nat. Methods*, 2011, **8**, 871–878.
13 D. Moser and H. Bales, *Sens. Actuators, A*, 1993, **37-38**, 33–34.
14 P-Y. Wang and M. S. Lu, *IEEE Sens. J.*, 2011, **11**, 3469–3475.
15 E. Forsen, G. Abadal, S. Ghatnekar-Nilsson, J. Teva, J. Verd, R. Sandberg, W. Svendsen, F. Perez-Murano, J. Esteve, E. Figueras, F. Campabadal, L. Montelius, N. Barniol and A. Boisen, *Appl. Phys. Lett.*, 2005, **87**, 043507.
16 M. L. Johnston, I. Kymissis and K. L. Shepard, *IEEE Sens. J.*, 2010, **10**, 1042–1047.
17 C. Hagleitner, A. Hierlemann, D. Lange, A. Kummer, N. Kerness, O. Brand and H. Baltes, *Nature*, 2011, **414**, 293–296.
18 P. M. Levine, P. Gong, R. Levicky and K. L. Shepard, *IEEE J. Solid-State Circuits*, 2008, **43**, 1859–1871.
19 S. Joo and R. B. Brown, *Chem. Rev.*, 2008, **108**, 638–651.
20 M. Schienle, C. Paulus, A. Frey, F. Hofmann, B. Holzapfl, P. Schindler-Bauer and R. Thewes, *IEEE J. Solid-State Circuits*, 2004, **39**, 2438–2445.
21 G. Li, V. Joshi, R. L. White, S. X. Wang, J. T. Kemp, C. Webb, R. W. Davis and S. Sun, *J. Appl. Phys.*, 2003, **93**, 7557–7559.
22 P. Besse, G. Boero, M. Demierre, V. Pott and R. Popovic, *Appl. Phys. Lett.*, 2002, **80**, 4199–4201.
23 T. Aytur, J. Foley, M. Anwar, B. Boser, E. Harris and P. R. Beatty, *J. Immunol. Methods*, 2006, **314**, 21–29.
24 P. Liu, K. Skucha, M. Megens and B. Boser, *IEEE Trans. Magn.*, 2011, **47**, 3449–3451.
25 H. Lee, E. Sun, D. Ham and R. Weissleder, *Nat. Med.*, 2008, **14**, 869–874.
26 H. Wang, Y. Chen, A. Hassibi, A. Scherer and A. Hajimiri, *IEEE ISSCC Dig. Tech.*, 2009, 438–439.
27 H. Wang, S. Kosai, S. Sideris and A. Hajimiri, *IEEE MTT-S Int. Microwave Symp. Dig.*, 2010, 616–619.
28 R. Matijevi, *Fine Particles in Medicine and Pharmacy*, Springer, 2011.
29 J. Llandro, J. J. Palfreyman, A. Ionescu and C. H. W. Barnes, *Med. Biol. Eng. Comput.*, 2010, **48**, 977–998.
30 K. R. Boheler, J. Czyz, D. Tweedie, H.-T. Yang, S. V. Anisimov and A. M. Wobus, *Circ. Res.*, 2002, **91**, 189–201.
31 A. Mahdavi, R. E. Davey, P. Bhola, T. Yin and P. W. Zandstra, *PLoS Comput. Biol.*, 2007, **3**, 1257–1267.
32 J. M. Karp, J. Yeh, G. Eng, J. Fukuda, J. Blumling, K.-Y. Suh, J. Cheng, A. Mahdavi, J. Borenstein, R. Langer and A. Khademhosseini, *Lab Chip*, 2007, **7**, 786–794.
33 R. E. Klabunde, *Cardiovascular Physiology Concepts*, Lippincott Williams & Wilkins, 2005.
34 D. Mohrman and L. Heller, *Cardiovascular Physiology*, McGraw-Hill Professional, 2010.
35 R. Gianelly, J. O. von der Groeben, A. P. Spivack and D. C. Harrison, *N. Engl. J. Med.*, 1967, **277**, 1215–1219.
36 J. B. Christen and A. G. Andreou, *IEEE Transactions on Biomedical Circuits and Systems*, 2007, **1**, 3–18.
37 J. El-Ali, P. K. Sorger and K. F. Jensen, *Nature*, 2006, **442**, 403–411.
38 E. Lauwers, J. Suls, W. Gumbrecht, D. Maes, G. Gielen and W. Sansen, *IEEE J. Solid-State Circuits*, 2001, **36**, 2030–2038.